

University of Texas Rio Grande Valley

ScholarWorks @ UTRGV

Physics and Astronomy Faculty Publications
and Presentations

College of Sciences

9-2-2014

Theoretical and experimental infrared spectra of hydrated and dehydrated sulfonated poly(ether ether ketone)

Jonathan Doan

Erin Kingston

Ian Kendrick

Kierstyn Anderson

N. Dimakis

The University of Texas Rio Grande Valley, nicholas.dimakis@utrgv.edu

See next page for additional authors

Follow this and additional works at: https://scholarworks.utrgv.edu/pa_fac



Part of the [Astrophysics and Astronomy Commons](#), and the [Physics Commons](#)

Recommended Citation

Doan, Jonathan, et al. "Theoretical and experimental infrared spectra of hydrated and dehydrated sulfonated poly (ether ether ketone)." *Polymer* 55.18 (2014): 4671-4676. <https://doi.org/10.1016/j.polymer.2014.07.011>

This Article is brought to you for free and open access by the College of Sciences at ScholarWorks @ UTRGV. It has been accepted for inclusion in Physics and Astronomy Faculty Publications and Presentations by an authorized administrator of ScholarWorks @ UTRGV. For more information, please contact justin.white@utrgv.edu, william.flores01@utrgv.edu.

Authors

Jonathan Doan, Erin Kingston, Ian Kendrick, Kierstyn Anderson, N. Dimakis, Philippe Knauth, Maria Luisa Di Vona, and Eugene S. Smotkina

Infrared spectroscopy of ion-induced cross-linked sulfonated poly(ether ether ketone)

Kierstyn Anderson¹, Erin Kingston¹, Joseph Romeo¹, Jonathan Doan¹, Neili Loupe¹, Nicholas Dimakis², Eugene S. Smotkin^{1*}

¹Department of Chemistry and Chemical Biology, Northeastern University, Boston MA 02115, USA

²Department of Physics, University of Texas Rio Grande Valley, Edinburg, TX 78539

KEYWORDS Cross-linking, SPEEK, Infrared spectroscopy

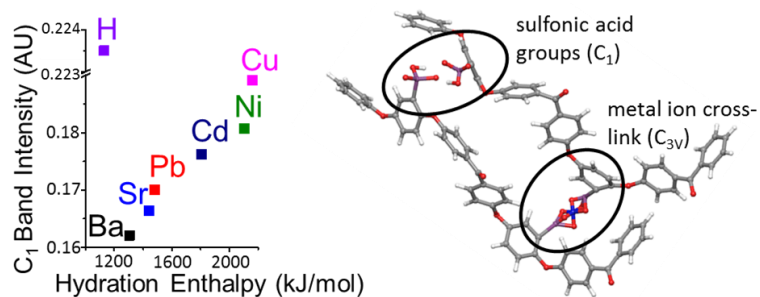
1 Abstract

2 The dehydration of SPEEK-[H] (protonated sulfonated poly(ether ether ketone)) converts
3 3-fold symmetric (C_{3V}) hydrated sulfonate sites to sulfonic acid sites with no local symmetry
4 (C_1). Like Nafion[®]-[H], SPEEK-[H] C_{3V} and C_1 environments afford IR group modes ($C_{3V,HF}$
5 (1087 cm^{-1}); $C_{3V,LF}$ (1026 cm^{-1}) and $C_{1,HF}$ (1362 cm^{-1}); $C_{1,LF}$ (904 cm^{-1})) due to the mechanical
6 coupling of vibrational internal coordinates of an ether link with those of the sulfonate or
7 sulfonic acid exchange site. C_{3V} and C_1 bands are inversely correlated during membrane
8 hydration/dehydration. Hydrated SPEEK-[M] (M: Cu^{2+} , Ni^{2+} , Cd^{2+} , Pb^{2+} , Sr^{2+} or Ba^{2+}) exhibits
9 SPEEK-[H] C_{3V} bands because cation waters of hydration preclude binding to the hydrated
10 exchange site. When cation hydration spheres are thermally stripped at high vacuum, SPEEK-
11 [M] C_{3V} bands supplant SPEEK-[H] C_{3V} bands, inducing SPEEK cross-linking. Incomplete
12 cross-linking is evidenced by low intensities of SPEEK-[M] $C_{1,HF}$ bands. The 1362 cm^{-1} band
13 intensities are inversely correlated with cation hydration enthalpies.

14

15

16



1 Graphical Abstract

2 Introduction

3 Nafion and sulfonated poly(ether ether ketone) (SPEEK) membranes (Fig. 1) are ideal for
 4 polymer electrolyte membrane (PEM) fuel cells because of the high proton conductivity afforded
 5 by sulfonate exchange groups ($-\text{SO}_3^-$) and their robust backbone structures.^{1,2,3} Nafion, a
 6 perfluorinated carbon backbone with vibrationally hinged (ether link) side chains that terminate
 7 with a sulfonate exchange site, has been the dominant PEM fuel cell electrolyte for several
 8 decades.⁴⁻⁶ Although Nafion has excellent chemical stability and proton conductivity,⁴ it is
 9 expensive, has diminished conductivity above 90°C ,^{4,7,8} is subject to a free radical catalyzed
 10 unzipping mechanism³ and generates fluorinated toxins when incinerated.^{9, 10} SPEEK is lower
 11 cost, has high chemical, thermal, and mechanical stability,^{1,7,11} and is environmentally
 12 friendly.^{12,2,3,13,14}

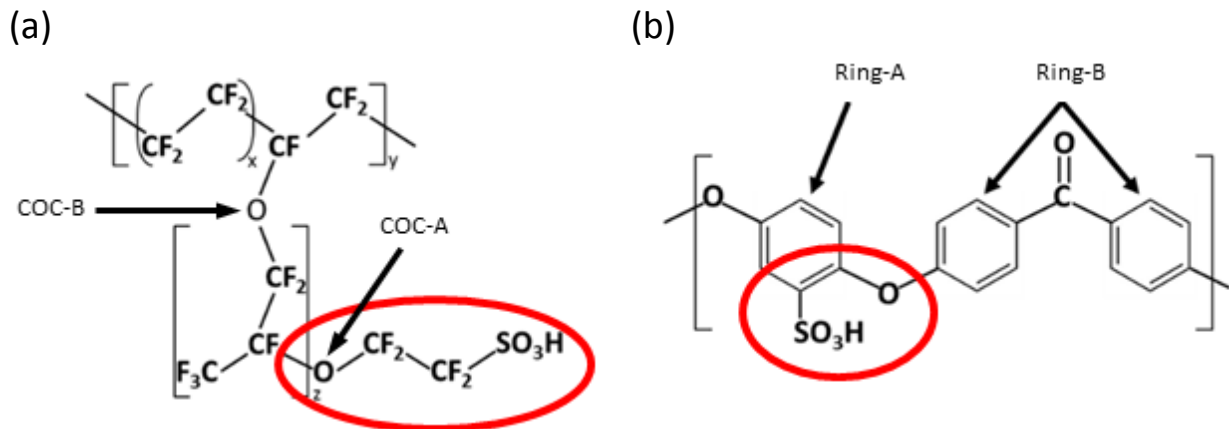
13 Differences in morphology and microstructure account for functional discrepancies (e.g.,
 14 proton conductivity, thermal stability) between SPEEK and Nafion.¹⁵ SPEEK has narrower
 15 aqueous channels and dead ended aqueous confines that result in lower proton conductivity than
 16 Nafion with the same degree of sulfonation.^{3,15} While proton conductivity increases with degree
 17 of sulfonation,^{14,16,17} membrane swelling also increases, diminishing mechanical strength.
 18 ^{1,2,12,13,15,11,18,19,20} Cross-linking mitigates much of the mechanical limitations imposed by higher

1 degrees of sulfonation^{8,13,11,18,20} to the extent that highly sulfonated cross-linked SPEEK can
2 outperform Nafion.^{21,22} Unfortunately the benefits of cross-linking^{8,13,19,20,21,22,23} come at the
3 expense of lower proton conductivity.¹⁹

4 SPEEK cross-linking methods are not well developed due to the rigid backbone structure.
5 SPEEK ether links are hampered vibrational hinges because their lone pair electrons are
6 delocalized by resonance. While most cross-linking strategies involve covalent bonding, ionic
7 bonding⁸ and a combination of both²⁰ have been explored. Chemical (covalent) cross-linking^{22, 24}
8 is done through electron beam irradiation,¹¹ UV irradiation,²³ free radical reactions or the use of
9 PEEK precursors that generate cross-linked products.⁸ Physical methods are less understood,²²
10 but provide facile methods for study of cross-linking. Ionic cross-linking is a physical method
11 that requires the maintenance of electrical neutrality.²² Narducci et al. suggest ionic cross-linking
12 by divalent ions in hydrated SPEEK membranes.²⁵ Cross-linking with Sr^{2+} and Ba^{2+} has been
13 reported.^{8, 22} Quezado et al. conducted a comprehensive FTIR study of metal ion-water
14 interactions in Nafion at low levels of hydration.²⁶ Their study of 20 cations at wavenumbers
15 above 1550 cm^{-1} showed that Lewis acid and base strengths of cations and anions are good
16 indicators of their affinity for each other and of the resistance of cation-anion pairs to disruption
17 by water molecules. Our recent report on interactions between cations and the exchange group,
18 in totally dehydrated Nafion, focused on wavenumbers below 1200 cm^{-1} : Strong binding
19 between cations and the dehydrated exchange group feature C_{3v} local symmetry with substantial
20 orbital overlap between the metal ion and the exchange site sulfur atom.²⁷ Our crystal orbital
21 overlap population calculations also showed a surprisingly high level of orbital overlap between
22 lithium and the exchange site sulfur.²⁷ This explains why lithium-exchanged sulfonated ionomers

1 are not good battery electrolytes.^{28, 29} Quezado et al. also reported anomalously strong
2 interactions between Li^+ and Nafion exchange sites.²⁶

3 The proximity of the exchange site to an ether link (Fig. 1, red circles) yields striking
4 similarities between Nafion and SPEEK vibrational spectroscopy. They both have IR group
5 modes derived from the mechanical coupling of the exchange site with a nearest neighbor ether
6 link (e.g., COC-A in the case of Nafion).³⁰ These IR group modes are categorized in terms of the
7 local symmetry of the exchange site, which depends on the state-of-hydration and the charge
8 compensating ion.^{3, 27, 30-33} When the membrane is hydrated, the exchange site is dissociated to
9 the sulfonate form and has a C_{3v} local symmetry. At lower states-of-hydration the exchange site
10 associates to a sulfonic acid form that has no local symmetry (i.e. C_1). Thus group modes that are
11 consequences of the mechanical coupling of the exchange site to the nearest neighbor ether link
12 are categorized as either C_{3v} or C_1 group modes.



13 Figure 1: Chemical repeat units of (a) Nafion and (b) SPEEK. The proximity of the ion exchange
14 site to an ether link³⁴ (circled in red) is common to both structures.

1 In Nafion-[H], the higher frequency C_{3V} mode (1060 cm^{-1}), referred to as $C_{3V,HF}$, is dominated by
2 COC-A motions that are mechanically coupled to the exchange site. The $C_{3V,LF}$ (969 cm^{-1}) is
3 dominated by exchange site motions coupled to a smaller COC-A contribution.³⁰⁻³² Proton
4 association during dehydration of Nafion-[H] yields the sulfonic acid form of the exchange site (-
5 SO_3H) which has no local symmetry (C_1).³ This gives rise to Nafion $C_{1,HF}$ (1414 cm^{-1}) and $C_{1,LF}$
6 (910 cm^{-1}) group modes, derived from the mechanically coupled internal coordinates of COC-A
7 and the $-\text{SO}_3\text{H}$ exchange site.²⁷

8 The assignment of IR bands attributed to the side chain of hydrated Nafion in terms of a
9 single functional group has led to enormous confusion.^{30, 35-37} For example, the 1060 cm^{-1} is
10 frequently assigned as a $-\text{SO}_3^{-1}$ mode. Similarly, the 969 cm^{-1} is assigned as a COC-A mode.^{30, 35,}
11 ³⁶ These single functional group assignments preclude understanding of why their band
12 intensities are strongly and inversely correlated to alterations of the exchange site environment.^{3,}
13 ^{27, 30-32} The assignment of these Nafion bands as local symmetry based *group* modes is paradigm
14 shift from decades of history: The 1060 cm^{-1} and 969 cm^{-1} bands are COC-A, $-\text{SO}_3^{-1}$ and COC-
15 A, $-\text{SO}_3^{-1}$ group modes respectively. Both modes are attributed to the same mechanically
16 coupled functional groups, which are listed in order of importance in their respective
17 assignments. The primary functional group contributors, in both modes, are the reverse of the
18 historical assignments.^{3, 27, 30, 31, 38, 39}

19 Proton and metal ion exchanged Nafion membranes are designated as Nafion-[H] and
20 Nafion-[M], respectively.²⁷ At high states-of-hydration the Nafion-[M] sulfonate exchange site
21 environment is spectroscopically indistinguishable from that of Nafion-[H] because cation waters
22 of hydration preclude direct binding of the cations to the exchange site.

1 The correlations of ionomer exchange site local symmetry, state-of-hydration, and ion-
2 exchange, to density functional theory (DFT) calculated normal modes and observed IR bands
3 would be better understood and reinforced if extended to other sulfonated ionomers.^{3, 30-32, 38, 40}
4 This work establishes symmetry-based IR group mode assignments for SPEEK-[H] and applies
5 them towards the analysis of dehydrated SPEEK-[M], where M is Cu²⁺, Ni²⁺, Cd²⁺, Pb²⁺, Sr²⁺ or
6 Ba²⁺.

1 **Experimental**

2 **Ion Exchange**

3 SPEEK Fumapem-E- 730 (Fumatech, Bietigheim-Bissingen, Germany) membranes were
4 used as is and soaked in 1M salt solutions (CdCl_2 , CuSO_4 , NiCl_2 , $\text{Pb}(\text{NO}_3)_2$, $\text{Ba}(\text{C}_2\text{H}_3\text{O}_2)_2$ and
5 $\text{Sr}(\text{C}_2\text{H}_3\text{O}_2)_2$) (48 hrs).

6 **Membrane Transmission FTIR spectroscopy**

7 SPEEK membranes were removed from solution, briefly rinsed with Nanopure™ water,
8 pat-dried with ChemWipes™, and placed in the Vertex 70 FT-IR spectrometer (Bruker, Billerica,
9 MA) to obtain the spectra of the fully hydrated membrane under ambient conditions. The sample
10 is then transferred into the Vertex 80 vacuum (1.00 hPa) spectrometer (Bruker, Billerica, MA),
11 enclosed within a custom glovebox, for time dependent spectra.³ Spectra were obtained every
12 half hour for one full day, and then hourly until a steady state condition was attained (12 – 60
13 hrs). Dehydration was continued on a high vacuum line (60°C, 2 days) equipped with a Welch
14 1402 DuoSeal vacuum pump, a glass oil diffusion pump (Ace Glass, Vineland, NJ) and a liquid
15 N_2 trap. After dehydration, the sample bulb was transferred to the FT-IR glove box, and the
16 membrane returned to the Vertex 80 sample chamber for acquisition of a final spectrum. Spectra
17 were signal averaged (50 scans, 4 cm^{-1} resolution) using a DLaTGS detector. Data processing
18 was completed using Bruker™ OPUS 6.5™ software.

19 **Attenuated Total Reflectance (ATR) Spectroscopy**

20 A MIRacle ATR accessory (Pike Technologies Spectroscopic Creativity, Madison, WI)
21 with a ZnSe ATR crystal was used, inserted into the Vertex 70 FT-IR spectrometer sample stage.
22 A surface pressure of 815 psi was maintained over the 1.8 mm diameter ATR crystal. The
23 spectra were signal averaged from 100 scans at 4 cm^{-1} resolution with a dry-air purge at ambient

1 temperature. Atmospheric compensation (to eliminate H₂O and CO₂ interference in the beam
2 path) was used in all measurements. Data processing for all infrared data was done with the
3 Bruker OPUS 6.5 software.

4 **PEEK sulfuric acid treatment**

5 A 20:1 vol/vol% solution of hexanes (reagent grade, Sigma-Aldrich) and fuming sulfuric
6 acid was shaken vigorously in a separation funnel to diffuse SO₃ into the hexanes. The organic
7 mixture (hexanes/SO₃), was then extracted from the acid layer. PEEK (2 x 0.75 cm, Novamem,
8 Zurich, Switzerland) was then submerged in the organic mixture for 6 min. The treated
9 membrane was then dried using Kim wipes and attached to microscope slides using double-sided
10 adhesive tape. ATR spectra were taken directly from the slide-mounted treated PEEK.

11 **Molecular Modeling Calculations**

12 Unrestricted DFT⁴¹ with the X3LYP⁴² functional was used for geometry optimizations
13 and calculations of the normal mode frequencies of PEEK repeat units. The X3LYP is an
14 extension to the B3LYP⁴³ functional providing more accurate heats of formation. The 80-atom
15 repeat unit consists of two PEEK monomer units plus an additional aromatic ring. Jaguar 8.7
16 (Schrodinger Inc., Portland, OR) was used with the all-electron 6-311G**++ Pople triple- ζ basis
17 set (“**” and “++” denote polarization⁴¹ and diffuse⁴⁴ basis set functions, respectively). Output
18 files were converted to vibrational mode animations using the Maestro graphical user interface
19 (Schrodinger Inc., New York, NY). Calculations were carried out on the high performance
20 computing cluster at the University of Texas Rio Grande Valley with 72 nodes of Dual 2.67 Ghz
21 processors; each node with 48 GB RAM and 250 GB disk. DFT-calculated normal mode peaks
22 are denoted by superscript (*) e.g. 983* cm⁻¹. Maestro animations for normal modes with
23 normalized intensity above 1% of the largest peak were selected for viewing.

1 **Results and Discussion**

2 **SPEEK-[H] vs. PEEK**

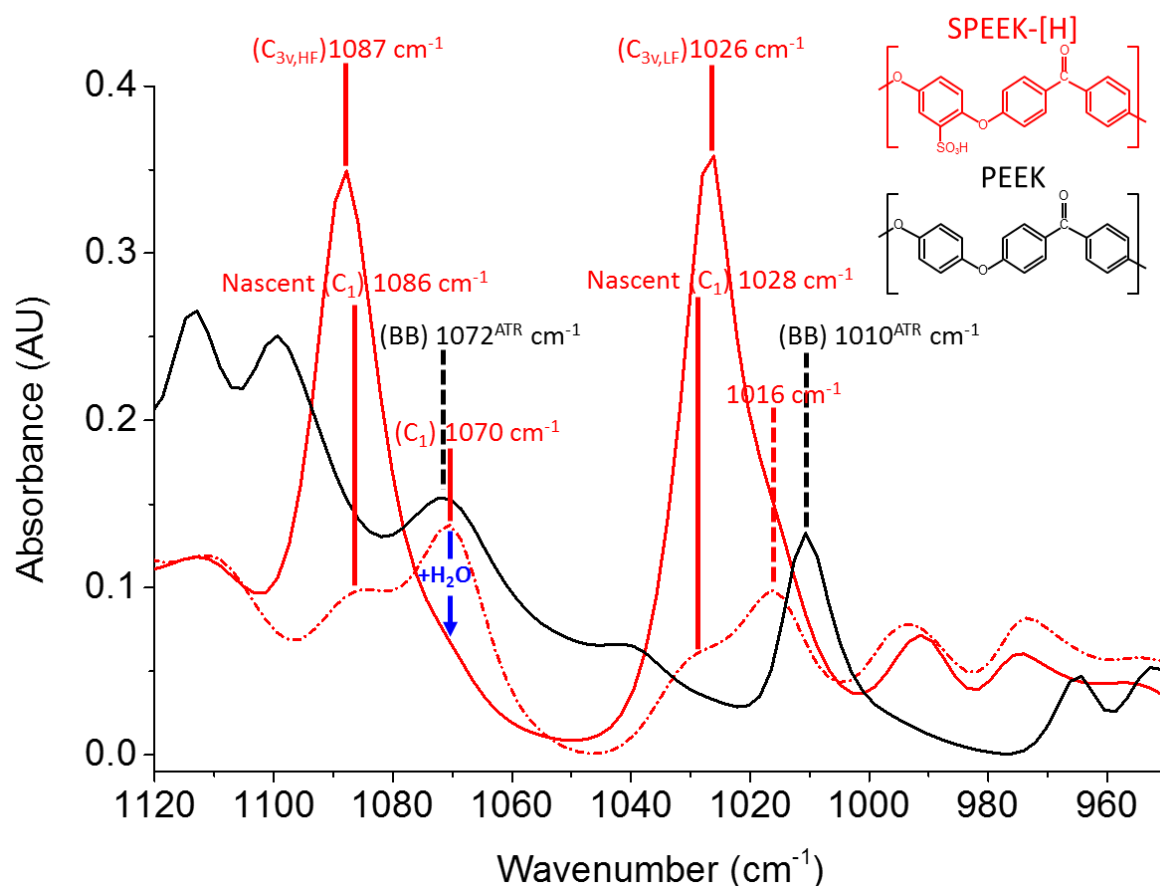
3 Correlation of theoretically calculated normal modes to observed IR bands is a simpler
4 matter for SPEEK than Nafion. SPEEK is an ionomer for which the entire “backbone” structure,
5 less the sulfonate group, is available as poly(ether ether ketone) (PEEK) (Fig. 2, black structure).
6 No such backbone analog for Nafion is commercially available.

7 Hopefully, the lessons learned from Nafion will preclude the assignments of hydrated
8 SPEEK-[H] 1087 cm^{-1} ($C_{3V,HF}$) and 1026 cm^{-1} ($C_{3V,LF}$) bands as single functional group modes.
9 They are C_{3V} group modes that involve mechanically coupled internal coordinates of both the
10 dissociated sulfonate exchange site (with a local three fold axis of symmetry) and the nearest
11 neighbor ether link (Fig. 1, red circle).

12 Figure 2 shows the transmission spectra of both hydrated (solid red) and dehydrated
13 (dashed red) SPEEK-[H], superimposed upon the PEEK ATR spectrum (black). In general, the
14 correlation of measured band frequencies to theoretically calculated normal modes requires
15 additional experiments.^{3, 30, 32, 45} For example, experimental confirmation that the PEEK 1072^{ATR}
16 cm^{-1} band corresponds to Ring-A was obtained by surface treatment of PEEK with sulfuric acid
17 saturated hexane. The Ring-A structure was substantially altered to the point of complete
18 disappearance of the peak at $1072^{\text{ATR}}\text{ cm}^{-1}$ (see Supplemental Figure S1).

19 The PEEK ATR spectrum shows backbone modes (BB) at $1010^{\text{ATR}}\text{ cm}^{-1}$ and 1072^{ATR}
20 cm^{-1} (black dashed vertical line highlights) which are substantially altered by sulfonation of
21 Ring-A (dashed red spectrum). The $1010^{\text{ATR}}\text{ cm}^{-1}$ backbone band shifts to the SPEEK-[H] band
22 at 1016 cm^{-1} . The 1016 cm^{-1} band, upon hydration of SPEEK-[H], is enveloped by the $C_{3V,LF}$
23 mode (solid red spectrum) and thus persists as a shoulder. The dehydrated SPEEK-[H] C_1 mode

1 at 1070 cm^{-1} is unrelated to the PEEK backbone mode at $1072^{\text{ATR}}\text{ cm}^{-1}$. In fact, the C_1 mode
 2 vanishes upon full hydration (blue arrow to solid red spectrum) while the $C_{3V,HF}$ and $C_{3V,LF}$
 3 appear at 1087 cm^{-1} and 1026 cm^{-1} (solid red vertical line highlights). IR spectra (from 1600 cm^{-1}
 4 to 800 cm^{-1}) of PEEK, dehydrated SPEEK-[H], and hydrated SPEEK-[H] with overlaid DFT-
 5 calculated normal modes are available in Supplemental Figure S2. Group mode PEEK and
 6 SPEEK-[H] band assignments were obtained by eigenvector visualization. (Table 1).^{3,30,31}



7 Figure 2. SPEEK-[H] transmission spectra (red): hydrated (solid), dehydrated (dashed). PEEK
 8 ATR spectrum (black). Dashed vertical lines highlight bands insensitive to the exchange site
 9 environment.

10

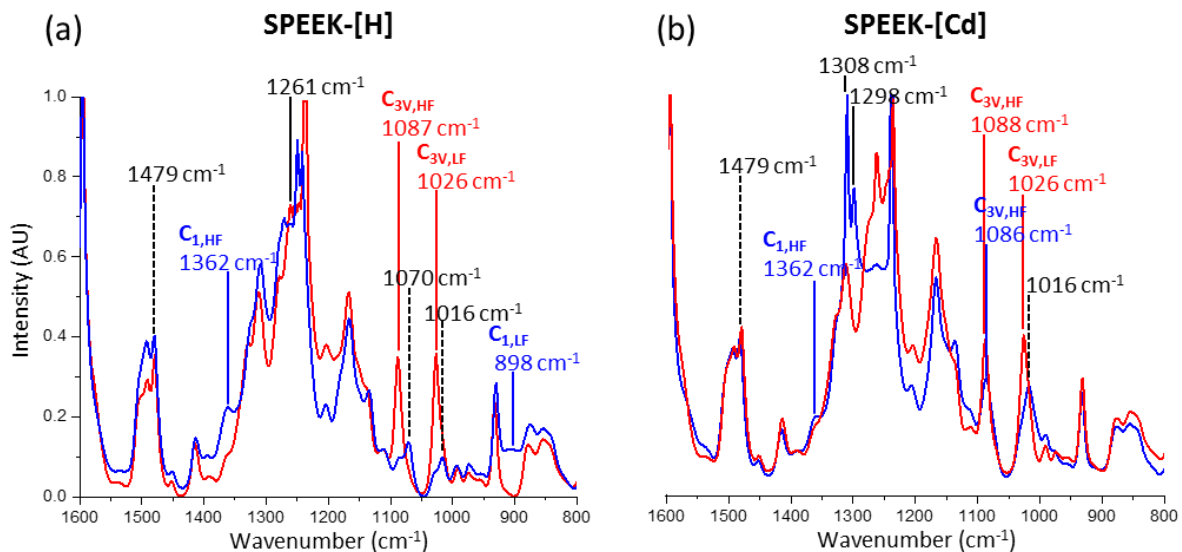
1 Dehydrated SPEEK-[H] has bands at 1086 cm^{-1} (1108^* cm^{-1}) and 1028 cm^{-1} (1069^* cm^{-1}).
2 ¹). These experimental bands are tentatively assigned as nascent C_1 bands (Fig. 2, dashed red
3 spectrum). Visualization of eigenvector animations show substantial contribution by the $-\text{SO}_3\text{H}$
4 form of the exchange site. The two bands are not yet experimentally confirmed as C_1 bands,
5 because $C_{3V,HF}$ and $C_{3V,LF}$ overlap at those wavenumbers and preclude definitive assignments. It
6 is hoped that further work, quantitatively decomposing DFT-calculated normal modes into pure
7 modes (i.e., individual vibrational motions of specific functional groups),⁴⁶ will allow
8 confirmation of the bands as C_1 group modes.

	Transmission (cm ⁻¹)	ATR (cm ⁻¹)	DFT (cm ⁻¹)	Normal mode components	Band Assignment
Hydrated Nafion-[H]	969	971 ^{ATR}	983*	SO ₃ ⁻ v _s , COC-A v _{as}	C _{3v,LF}
	1061	1056 ^{ATR}	1059*	COC-A v _{as} , v _s SO ₃ ⁻	C _{3v,HF}
Dehydrated Nafion-[H]	910		786*	SO ₃ H v _s , COC-A v _s	C _{1,LF}
	1414		1405*	SO ₃ H v _{as} , COC-A v _{as}	C _{1,HF}
Hydrated SPEEK-[H]	1016		943*	Φ _{b,OOP} , C=O δ _s v _s , CH _b v _{as}	C _{3v,LF}
	1026	1020 ^{ATR}	981*	Φ _{a,IP} , SO ₃ ⁻ v _s	
	1087	1076 ^{ATR}	1029* 1068*	Φ _{a,IP} , CH _a v _{as} Φ _{a,IP} , CH _a v _{as} , SO ₃ ⁻ v _s	C _{3v,HF}
Dehydrated SPEEK-[H]	898		769*	Φ _{a,OOP} , Φ _{b,OOP} , SO ₃ H v _s	C _{1,LF}
	1016		959*	C=O δ _s v _s , Φ _{b,OOP} , CH _b v _{as}	Nascent C ₁
	1028		1069*	Φ _{a,IP} , SO ₃ H v _{as} , CH _a v _{as}	
	1070		1071*	SO ₃ H v _{as} , Φ _{b,IP} , Φ _{a,IP}	C ₁
	1086		1108*	Φ _{a,IP} , SO ₃ H v _{as}	Nascent C ₁
	1362		1374*	Φ _{a,IP} , Φ _{b,IP} , SO ₃ H v _{as}	C _{1,HF}
PEEK		1010 ^{ATR}	944*	Φ _{b,OOP} , C=O δ _s v _s , CH _b v _{as}	BB
		1072 ^{ATR}	1032*	Φ _{a,IP} , CH _a v _{as}	BB

1 Table 1 – Transmission, ATR, and DFT-calculated normal modes for Nafion-[H] (hydrated and
2 dehydrated), SPEEK-[H] (hydrated and dehydrated), and PEEK. Subscripts a and b refer to Ring
3 a and Ring b. v_{as}: asymmetric stretching. v_s: symmetric stretching. δ_s: bending, δ_u: umbrella
4 bending. Φ: ring deformation. OOP: out of plane. IP: in plane. BB: backbone.

1 SPEEK-[H] vs. SPEEK-[M]

2 Figure 3(a) shows transmission spectra of hydrated SPEEK-[H] (red) and dehydrated
3 SPEEK-[H] (blue). The transition of the exchange site local symmetry from C_{3V} to C_1 is
4 evidenced by the complete loss of the C_{3V} bands (red line highlights) concomitant with the
5 emergence of the $C_{1,LF}$ at 898 cm^{-1} and the $C_{1,HF}$ at 1362 cm^{-1} (blues line highlights). Figure 3(b)
6 shows superimposed fully hydrated (red) SPEEK-[Cd] and dehydrated (blue) spectra. In SPEEK-
7 [Cd] spectra, a $C_{3V,LF}$ band persists at all states-of-hydration. At high states of hydration, the
8 exchange site is essentially a hydrated SPEEK-[H] environment because the cations are screened
9 from the exchange site. As the membrane is dehydrated, the sulfonate $C_{3V,LF}$ at 1026 cm^{-1}
10 transitions to a Cd^{2+} complexed sulfonate $C_{3V,LF}$ at 1016 cm^{-1} . The Cd^{2+} resides in the sulfur
11 trioxide pocket,²⁷ with substantial orbital overlap with the sulfur atom. The small $C_{1,HF}$ shoulder
12 at 1362 cm^{-1} suggests trace amounts of sulfonic acid (C_1) groups. A SPEEK-[Cd] $C_{1,LF}$,
13 analogous to the SPEEK-[H] $C_{1,LF}$ at 898 cm^{-1} , is never observed.



14 Figure 3. SPEEK transmission spectra: hydrated (red), dehydrated (blue). (a) SPEEK-[H]. (b)
15 SPEEK-[Cd].

1 Transmission spectra for SPEEK-[H] and SPEEK-[M] (Cu^{2+} , Ni^{2+} , Cd^{2+} , Pb^{2+} , Sr^{2+} and
2 Ba^{2+}) are shown in Figure 4(a) and 4(b), in order of cation hydration enthalpy. For greater detail,
3 transmission spectra of superimposed hydrated/dehydrated SPEEK-[M] are in Supplemental
4 Figures S4-S8. The spectra of fully hydrated SPEEK-[M] all show “hydrated” SPEEK-[H] $\text{C}_{3\text{V}}$
5 features irrespective of the cation, because cation hydration spheres preclude direct binding to
6 the exchange site (Fig. 4a).

7 During SPEEK-[M] dehydration, cation hydration spheres are stripped away enabling
8 direct binding of cations to the exchange site: SPEEK-[M] $\text{C}_{3\text{V}}$ bands emerge at the expense of
9 the SPEEK-[H] $\text{C}_{3\text{V}}$ bands (Fig. 4a to 4b). A rescaled inset (Fig. 4e) shows that the $\text{C}_{1,\text{LF}}$ band
10 appears in SPEEK-[H] but is not observed in any of the SPEEK-[M] spectra. However, C_1
11 symmetry is not completely absent from SPEEK-[M] spectra. The dehydrated SPEEK-[M] $\text{C}_{1,\text{HF}}$
12 (Fig. 4c) intensity grows with increasing hydration enthalpy. Figure 4(d) highlights this
13 remarkable trend: Hydration spheres of ions with large hydration enthalpies are so difficult to
14 strip, that maximally dehydrated membranes continue to exhibit some SPEEK-[H] $\text{C}_{1,\text{HF}}$ band
15 intensity.

16

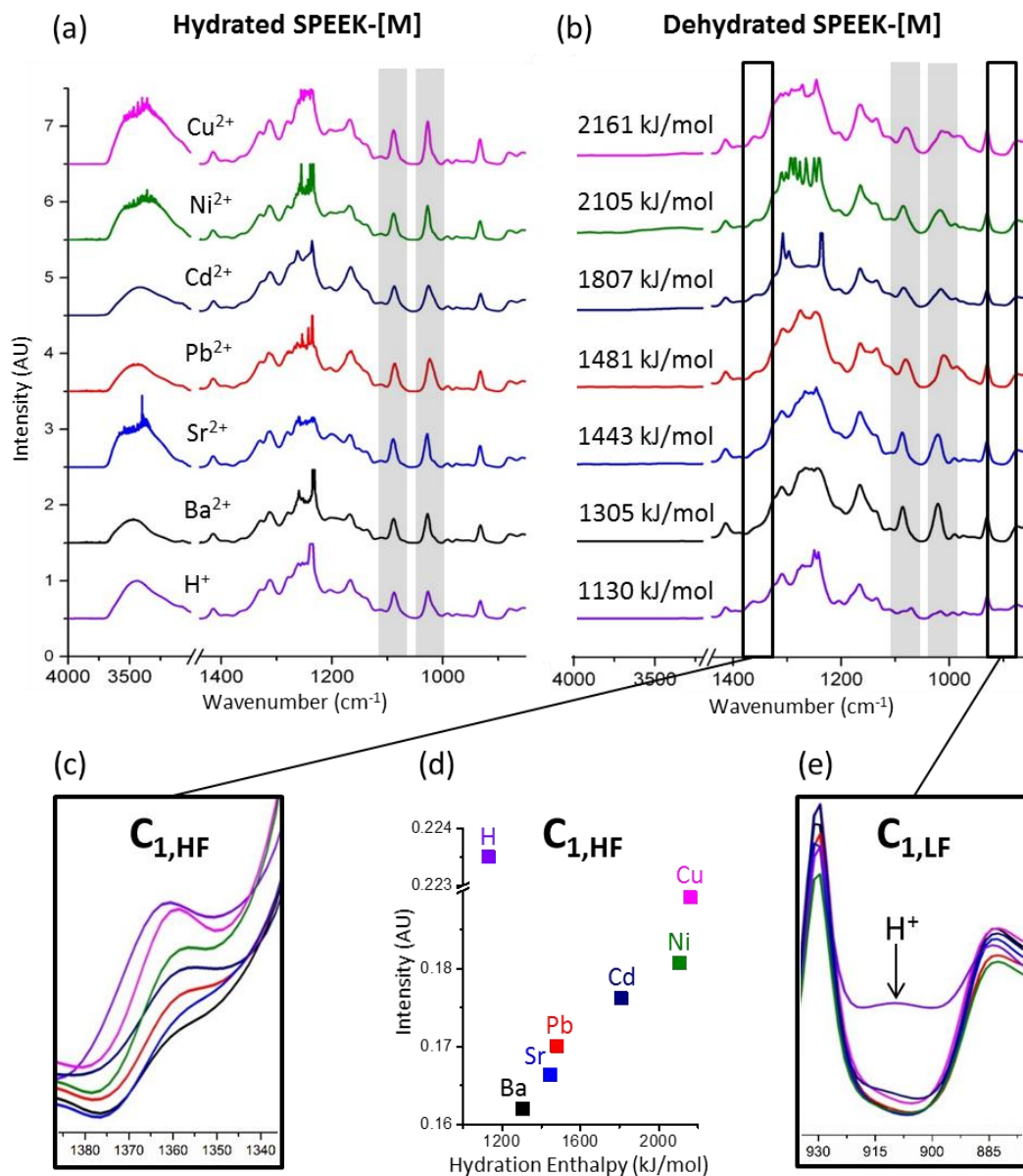
17

18

19

20

21



1 Figure 4. SPEEK-[M] transmission spectra: (a) hydrated, (b) dehydrated. (c) Highlighted C_{1,HF}
 2 band. (d) C_{1,HF} band intensity versus metal ion hydration enthalpy. (g) Highlighted C_{1,LF} band.

1 The tabulated SPEEK-[M] C_{3V} bands (Table 2) confirm the overwhelming presence of a
 2 local C_{3V} symmetry at the dehydrated SPEEK-[M] exchange site. This can be considered with
 3 respect to charge balance. An exchange site - divalent ion pair yields a net positive charge that
 4 can be formally charge balanced by (1) another cross-linking exchange site or (2) a hydroxide
 5 ion.

6 Hydroxide balancing yields a proton (from H_2O) that, during dehydration, will bind to an
 7 exchange site with C_1 symmetry. The presence of the low intensity SPEEK-[M] $C_{1,HF}$ band
 8 suggests low levels of hydroxide ion balancing. Figure 5 is a model of SPEEK that shows both a
 9 metal ion cross-link and sulfonic acid groups.

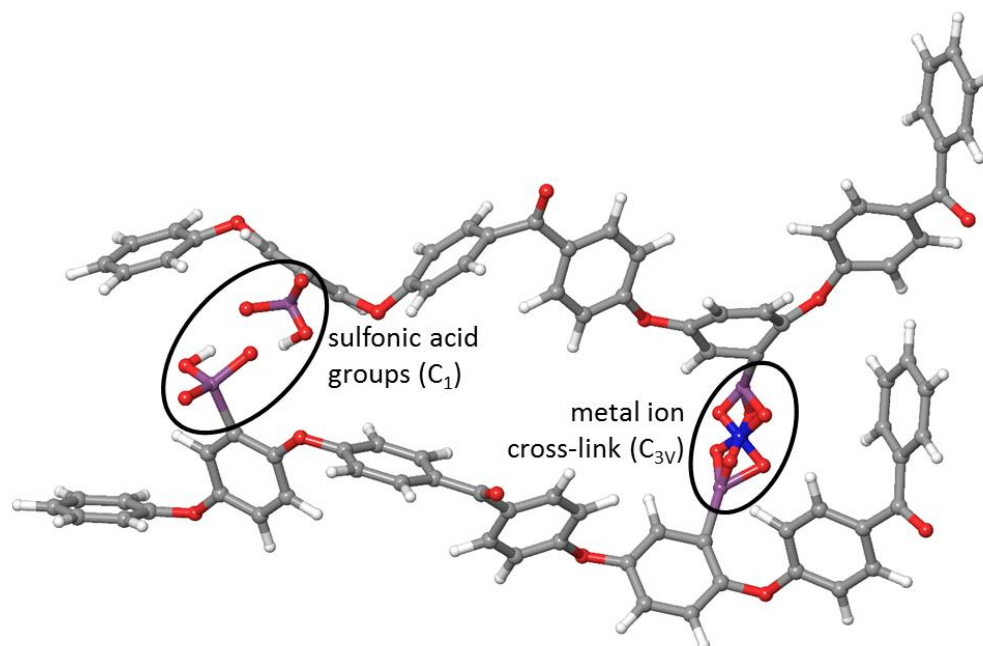
Ions	$-\Delta H_{Hyd}$ (kJ/mol)	Hydrated (cm^{-1})		Dehydrated (cm^{-1})		Figure
		$C_{3V, HF}$	$C_{3V, LF}$	$C_{3V, HF}$	$C_{3V, LF}$	
Cu^{2+}	2161	1088	1026	1080	-	S3
Ni^{2+}	2105	1089	1028	1084	-	S4
Cd^{2+}	1807	1088	1026	1086	-	3b
Pb^{2+}	1481	1087	1024	1080	-	S5
Sr^{2+}	1443	1089	1028	1088	1020	S6
Ba^{2+}	1305	1088	1027	1086	1022	S7
H^+	1130	1087	1026	-	-	3a

10 Table 2 –Ion-exchanged SPEEK C_{3V} transmission bands listed with ion hydration enthalpy.

11 Figures S3-S8 are in Supplementary Data.

12

13



1 Figure 5: Model of SPEEK-[M] with sulfonic acid groups and a metal ion cross-link. Carbon
 2 (gray), Oxygen (red), Sulfur (purple), Metal ion (blue).

3 The degree of cross-linking is expected to be inversely correlated to the SPEEK-[M]
 4 $C_{1,HF}$ band intensity. The $C_{1,HF}$ band intensity versus cation hydration enthalpy is shown in Fig.
 5 4d. Ions with low hydration enthalpy, such as Ba^{2+} , Sr^{2+} , and Pb^{2+} , have smaller $C_{1,HF}$ bands (i.e.,
 6 strong metal ion – exchange site interactions and less likelihood of the sulfonic acid form of the
 7 exchange site), resulting from a large degree of cross-linking. Cations with higher hydration
 8 enthalpies (Cd^{2+} , Ni^{2+} and Cu^{2+}) bind weakly to the exchange site. The exchange site cannot
 9 compete with waters of hydration, resulting in fewer cross-links.²² Gasa et al. showed that Ba^{2+}
 10 cation cross-linking renders a sulfonated ionomer less capable of water swelling as a function of
 11 methanol-water activity.²² Luu et al. continued by stating the reduction in water uptake was
 12 associated with the reduced ion cluster size revealed by small angle X-ray scattering analysis of
 13 Sr^{2+} ion-exchanged SPEEK.⁸ The reported enhanced cross-linking capabilities of Ba^{2+} and Sr^{2+}
 14 correlate with their positions in Fig. 4d.^{8, 22} The lower hydration enthalpy of Ba^{2+} and Sr^{2+} enable
 15 SPEEK-[M] exchange sites to successfully compete with hydration waters and thus yield brittle,

1 cross-linked²⁰ membranes.

2 The categorizations of IR group modes in terms of the local symmetry of the ion
3 complexing site can be extended beyond organic structures. There are reports of C_{3V} quasilattice
4 site symmetries in molten metal sulfates having two sulfates specifically associated with each
5 divalent metal ion.⁴⁷

6 **Conclusion**

7 The dissociated sulfonate exchange site of fully hydrated SPEEK-[H] has a local C_{3V}
8 symmetry. The vibrational normal mode internal coordinates of the sulfonate group are
9 mechanically coupled to the nearest neighbor ether link giving rise to a $C_{3V,LF}$ band at 1026 cm^{-1}
10 and the higher frequency $C_{3V,HF}$ at 1087 cm^{-1} . Infrared spectra of fully hydrated SPEEK-[H] and
11 SPEEK-[M], where M are divalent cations, are spectroscopically indistinguishable, because
12 cation waters of hydration shield the cation from the sulfonate exchange site inner sphere (i.e.,
13 hydrated SPEEK-[M] exhibits the SPEEK-[H] C_{3V} modes). When SPEEK-[H] is dehydrated, the
14 exchange site associates to the sulfonic acid form ($-\text{SO}_3\text{H}$), which has no local symmetry (C_1).
15 When SPEEK-[M] undergoes dehydration, the ion hydration spheres are stripped away, and the
16 SPEEK-[M] C_{3V} bands supplant SPEEK-[H] C_{3V} bands. Divalent cations bind to exchange sites
17 and induce cross-linking with C_{3V} local symmetry at the exchange sites. For all metals of this
18 study, a minority of exchange sites within SPEEK-[M] remain protonated when the membrane is
19 dehydrated. This yields low intensity SPEEK-[M] $C_{1,HF}$ bands at $\sim 1360\text{ cm}^{-1}$ with intensities (1)
20 directly correlated to the cation hydration enthalpy and (2) negatively correlated to the extent of
21 membrane cross-linking. As expected, the SPEEK-[M] $C_{1,HF}$ band range is centered around the
22 SPEEK-[H] $C_{1,HF}$ band at 1362 cm^{-1} .

- 1 1. X. F. Li, Z. Wang, H. Lu, C. J. Zhao, H. Na and C. Zhao, *Journal of Membrane Science*, 2005, **254**,
2 147-155.
- 3 2. V. R. Hande, S. K. Rath, S. Rao and M. Patri, *Journal of Membrane Science*, 2011, **372**, 40-48.
- 4 3. J. Doan, E. Kingston, I. Kendrick, K. Anderson, N. Dimakis, P. Knauth, M. L. Di Vona and E. S.
5 Smotkin, *Polymer*, 2014, **55**, 4671-4676.
- 6 4. E. Negro, M. Vittadello, K. Vezzu, S. J. Paddison and V. Noto, *Solid State Ionics*, 2013, **252**, 84-92.
- 7 5. G. Hougham, *Fluoropolymers 1*, Springer, 1999.
- 8 6. L. Liberti and F. G. Helfferich, *Mass transfer and kinetics of ion exchange*, Springer, 1983.
- 9 7. A. Basile, L. Paturzo, A. Iulianelli, I. Gatto and E. Passalacqua, *Journal of Membrane Science*,
10 2006, **281**, 377-385.
- 11 8. D. X. Luu and D. Kim, *Solid State Ion.*, 2011, **192**, 627-631.
- 12 9. S. H. de Almeida and Y. Kawano, *Journal of Thermal Analysis and Calorimetry*, 1999, **58**, 569-577.
- 13 10. C. Bas, L. Flandin, A. S. Danero, E. Claude, E. Rossinot and N. D. Alberola, *Journal of Applied*
14 *Polymer Science*, 2010, **117**, 2121-2132.
- 15 11. J. M. Song, J. Shin, J. Y. Sohn and Y. C. Nho, *Macromolecular Research*, 2011, **19**, 1082-1089.
- 16 12. R. Narducci, M. L. Di Vona and P. Knauth, *Journal of Membrane Science*, 2014, **465**, 185-192.
- 17 13. S. G. Feng, Y. M. Shang, G. S. Liu, W. Q. Dong, X. F. Xie, J. M. Xu and V. K. Mathur, *Journal of*
18 *Power Sources*, 2010, **195**, 6450-6458.
- 19 14. T. Yang and C. Liu, *International Journal of Hydrogen Energy*, 2011, **36**, 5666-5674.
- 20 15. X. Wu, X. Wang, G. He and J. Benziger, *Journal of Polymer Science Part B-Polymer Physics*, 2011,
21 **49**, 1437-1445.
- 22 16. Y. Paik, S. A. Chae, O. H. Han, S. Y. Hwang and H. Y. Ha, *Polymer*, 2009, **50**, 2664-2673.
- 23 17. S. Xue and G. Yin, *Polymer*, 2006, **47**, 5044-5049.
- 24 18. N. Zhang, G. Zhang, D. Xu, C. Zhao, W. Ma, H. Li, Y. Zhang, S. Xu, H. Jiang, H. Sun and H. Na,
25 *International Journal of Hydrogen Energy*, 2011, **36**, 11025-11033.
- 26 19. Y.-S. Ye, Y.-C. Yen, C.-C. Cheng, W. Y. Chen, L.-T. Tsai and F.-C. Chang, *Polymer*, 2009, **50**, 3196-
27 3203.
- 28 20. H. Y. Hou, B. Maranesi, J. F. Chailan, M. Khadhraoui, R. Polini, M. L. Di Vona and P. Knauth,
29 *Journal of Materials Research*, 2012, **27**, 1950-1957.
- 30 21. M. L. Di Vona, L. Pasquini, R. Narducci, K. Pelzer, A. Donnadio, M. Casciola and P. Knauth, *Journal*
31 *of Power Sources*, 2013, **243**, 488-493.
- 32 22. J. V. Gasa, R. A. Weiss and M. T. Shaw, *Journal of Membrane Science*, 2007, **304**, 173-180.
- 33 23. S. Zhong, X. Cui, H. Cai, T. Fu, C. Zhao and H. Na, *Journal of Power Sources*, 2007, **164**, 65-72.
- 34 24. M. L. Di Vona, G. Alberti, E. Sgreccia, M. Casciola and P. Knauth, *International Journal of*
35 *Hydrogen Energy*, 2012, **37**, 8672-8680.
- 36 25. R. Narducci, M. Di Vona and P. Knauth, *J. Membr. Sci.*, 2014, **465**, 185-192.
- 37 26. S. Quezado, J. C. T. Kwak and M. Falk, *Canadian Journal of Chemistry*, 1984, **62**, 958-966.
- 38 27. J. Doan, N. E. Navarro, D. Kumari, K. Anderson, E. Kingston, C. Johnson, A. Vong, N. Dimakis and
39 E. S. Smotkin, *Polymer*, 2015, **73**, 34-41.
- 40 28. H. Y. Liang, X. P. Qiu, S. C. Zhang, W. T. Zhu and L. Q. Chen, *Journal of Applied Electrochemistry*,
41 2004, **34**, 1211-1214.
- 42 29. R. R. Garsuch, D. B. Le, A. Garsuch, J. Li, S. Wang, A. Farooq and J. R. Dahn, *J. Electrochem. Soc.*,
43 2008, **155**, A721-A724.
- 44 30. M. Webber, N. Dimakis, D. Kumari, M. Fuccillo and E. S. Smotkin, *Macromolecules*, 2010, **43**,
45 5500-5502.
- 46 31. I. Kendrick, D. Kumari, A. Yakaboski, N. Dimakis and E. S. Smotkin, *J. Am. Chem. Soc.*, 2010, **132**,
47 17611-17616.

- 1 32. I. Kendrick, A. Yakaboski, E. Kingston, J. Doan, N. Dimakis and E. S. Smotkin, *J. Polym. Sci. Pt. B-*
2 *Polym. Phys.*, 2013, **51**, 1329-1334.
- 3 33. I. Kendrick, J. Doan and E. S. Smotkin, in *Vibrational Spectroscopy at Electrified Interfaces*, eds. A.
4 Wieckowski, C. Korzeniewski and B. Braunschweig, 2013, pp. 327-344.
- 5 34. E. Gonzalez, J. Arbiol and V. F. Puntès, *Science*, 2011, **334**, 1377-1380.
- 6 35. D. S. Warren and A. J. McQuillan, *J. Phys. Chem. B*, 2008, **112**, 10535-10543.
- 7 36. K. M. Cable, K. A. Mauritz and R. B. Moore, *Journal of Polymer Science, Part B: Polymer Physics*,
8 1995, **33**, 1065-1072.
- 9 37. Y. Q. Wang, Y. Kawano, S. R. Aubuchon and R. A. Palmer, *Macromolecules*, 2003, **36**, 1138-1146.
- 10 38. I. Kendrick, J. Fore, J. Doan, A. Vong, N. Loupe, M. Diem and E. S. Smotkin, *Journal of The*
11 *Electrochemical Society. In Press*, 2016, **163**.
- 12 39. N. Loupe, J. Doan and E. S. Smotkin, Manuscript Submitted, 2016.
- 13 40. N. Loupe, J. Doan and E. Smotkin, *Submitted to Catalysis Today on December 13*, 2015.
- 14 41. P. Hohenberg and W. Kohn, *Physical Review*, 1964, **136**, B864-B871.
- 15 42. X. Xu, Q. S. Zhang, R. P. Muller and W. A. Goddard, *Journal of Chemical Physics*, 2005, **122**, 14.
- 16 43. A. D. Becke, *Journal of Chemical Physics*, 1993, **98**, 5648-5652.
- 17 44. W. Kohn and L. J. Sham, *Physical Review*, 1965, **140**, A1133-A1138.
- 18 45. D. I. Bower and W. F. Maddams, *The Vibrational Spectroscopy of Polymers*, Cambridge University
19 Press, Cambridge, 1989.
- 20 46. J. Doan, T. Mion, I. Kendrick, A. Yakaboski, D. Kumari, A. Vong, N. Dimakis and E. S. Smotkin,
21 Manuscript in preparation, 2015.
- 22 47. R. Hester and K. Krishnan, *The Journal of Chemical Physics*, 1968, **49**, 4356-4360.

23